RSC Advances



PAPER

View Article Online

View Journal | View Issue



Cite this: RSC Adv., 2018, 8, 9017

Synthesis and characterisation of $Ba(Zn_{1-x}Co_x)_2Si_2O_7$ (0 $\leq x \leq$ 0.50) for blue-violet inorganic pigments

Takashi Tsukimori, Yusuke Shobu, Ryohei Oka and Toshiyuki Masui 🕩 *

Ba(Zn_{1-x}Co_x)₂Si₂O₇ ($0 \le x \le 0.50$) solid solutions were synthesized as novel blue-violet inorganic pigments by a conventional solid-state reaction method. The crystal structure, optical properties, and colour of the pigments were characterized. All the pigments were obtained in a single-phase form. The pigments strongly absorbed visible light at wavelengths from 550 to 650 nm, corresponding to the range of green to orange light. This optical absorption was caused by the d-d transition of the tetrahedrally coordinated Co^{2+} ($^4A_2(F) \rightarrow ^4T_1(P)$), which was the origin of the blue-violet colour of the pigments. The most intense colour was obtained for Ba(Zn_{0.85}Co_{0.15})₂Si₂O₇, where $a^* = +52.2$ and $b^* = -65.5$ in the CIE (Commission Internationale de l'Éclairage) $L^*a^*b^*$ system. These absolute values were significantly larger than those of commercial violet pigments such as $Co_3(PO_4)_2$ ($a^* = +33$ and $b^* = -32$) and $NH_4MnP_2O_7$ ($a^* = +39$ and $b^* = -21$). Therefore, the Ba(Zn_{0.85}Co_{0.15})₂Si₂O₇ pigment could be a novel blue-violet inorganic pigment.

Received 5th January 2018 Accepted 23rd February 2018

DOI: 10.1039/c8ra00101d

rsc li/rsc-advances

Introduction

Cobalt (Co) and its compounds have been applied in alloys, paints, catalysts, cements and ceramic pigments. $^{1-5}$ In particular, the $\mathrm{Co^{2^+}}$ ion is often employed as a colouring source for blue and violet pigments. There are a number of reports on blue pigments using $\mathrm{Co^{2^+}}$ ions, such as $\mathrm{Co_2SiO_4}$ olivine, 6 (Co, $\mathrm{Zn)_2SiO_4}$ willemite, 7 $\mathrm{CoAl_2O_4}$ spinel and $\mathrm{Co_2SnO_4}$. The colouring performance of these pigments mainly depends on the coordination number around the $\mathrm{Co^{2^+}}$ ion, which is very important for the appearance of the bluish colour. However, the use of a large amount of Co increases the cost of the material, which becomes expensive because of its rarity.

Accordingly, selection of an appropriate host lattice, minimization of the Co content and strong colouring performance are necessary, when Co is applied to colour pigments. Although many studies on the reduction of the amount of Co in the pigments have been reported, ¹⁰⁻¹⁴ almost of them are on the blue pigments and there are only a few reports on the violet pigments. ^{13,15,16}

Generally, the colour of inorganic pigments is mainly affected by the crystal field, generated by the ions surrounding the chromophore. Cobalt violet $(\text{Co}_3(\text{PO}_4)_2)$ and manganese violet $(\text{NH}_4\text{MnP}_2\text{O}_7)$ has been well known as current commercial violet pigments. The structure of $\text{Co}_3(\text{PO}_4)_2$ is formed by distorted trigonal bipyramids CoO_5 , fairly regular CoO_6

Department of Chemistry and Biotechnology, Graduate School of Engineering, Tottori University, 4-101, Koyama-cho Minami, Tottori 680-8552, Japan. E-mail: masui@chem.tottori-u.ac.jp; Fax: +81-857-31-5264; Tel: +81-857-31-5264

octahedra and almost regular PO₄ tetrahedra. Generally, cobalt ion can take various coordination numbers and represent various colours in phosphates, In Co₃(PO₄)₂·8H₂O, Co²⁺ has octahedral 6 coordination to show reddish violet colour, while in KCoPO4 it has tetrahedral 4 coordination to evince blue-violet colour. On the other hand, NH₄MnP₂O₇ presents violet colour due to the d-d transition of the octahedral coordinated Mn3+.18 However, the vividness of the Co3(PO4)2 and the NH₄MnP₂O₇ pigments is insufficient, that is, their absolute values of a^* and b^* in the CIE $L^*a^*b^*$ system are not so large. In this system, the parameter L^* indicate the brightness or darkness of a colour on relation to a neutral grey scale, while the parameters a^* (the red-green axis) and b^* (the yellow-blue axis) express the colour qualitatively. In addition, the thermal resistance of NH₄MnP₂O₇ is not enough, because it is decomposed around 340 °C.18 Some violet pigments without Co have been proposed recently, 19-21 but their colours are not much different from those of the existing commercial violet pigments. Organic pigments are inferior to inorganic pigments in heat resistance and weather resistance. Thus, it is significant to synthesize a novel violet inorganic pigment in which the colour property is improved.

Because of this situation, we focused on barium zinc silicate $BaZn_2Si_2O_7$ as a host lattice of the novel violet pigment. This compound has a layered structure composed of $[ZnO_4]^{2-}$ tetrahedra connected at each corner to $[SiO_4]$ tetrahedra. Each $[SiO_4]$ tetrahedron is connected over three corners to one $[SiO_4]$ and two $[ZnO_4]^{2-}$ tetrahedra, and the forth corner is a non-bridging oxygen atom. The Ba^{2+} ions are located in between the zinc silicate layers. 22,23 As a related compound, Ba(M,

RSC Advances

 $Ni)_2Si_2O_7$ (M = Zn or Mg) pigments have been ever reported, but they exhibit red and purplish red colours due to the d-d transition of the tetrahedral coordinated Ni2+.24 In this study, Ba($Zn_{1-x}Co_x$)₂Si₂O₇ ($0 \le x \le 0.50$) pigments were synthesized by a conventional solid-state reaction method, and the colour properties of the pigments were investigated as novel blue-violet inorganic pigments.

Experimental

Materials and methods

The Ba $(Zn_{1-x}Co_x)_2Si_2O_7$ (0 $\leq x \leq 0.50$) pigments were synthesized by a conventional solid-state reaction method. BaCO₃ (Kishida Chemical, Japan), ZnO (Kishida Chemical, Japan), SiO₂ (Wako Pure Chemical, Japan) and Co₃O₄ (Wako Pure Chemical, Japan) were used as starting materials. The raw materials were mixed in a stoichiometric amount in an agate mortar. The mixture was calcined in an alumina boat at 1250 °C for 6 h. The samples were ground in an agate mortar before characterisation.

Characterisation

The composition of the samples was confirmed by X-ray fluorescence spectroscopy (XRF; Rigaku, ZSX Primus). The crystal structures of the samples were identified by X-ray powder diffraction (XRD; Rigaku, Ultima IV) with Cu-Ka radiation (40 kV, 40 mA). The sampling width and the scan speed were 0.02° and 6.0 min⁻¹, respectively. The lattice parameters and volumes were calculated from the XRD peak angles, which were refined using α-Al₂O₃ as a standard and using the CellCalc Ver. 2.20 software. The size and morphology of the Ba(Zn_{0.85}Co_{0.15})₂Si₂O₇ particles were observed by using scanning electron microscopy (SEM; JEOL, JSM-6701F). Gold was sputtered before observation to avoid the charge-up of the samples. The purity of the samples was analysed by energy dispersive X-ray analysis (EDX; Oxford Instruments, INCA Energy). An X-ray photoelectron spectrum (XPS; ULVAC-PHI, PHI5000 VersaProve II) of the Ba(Zn_{0.85}-Co_{0.15})₂Si₂O₇ pigment was measured using Mg-Kα radiation to investigate the oxidation state of the Co ion.

The optical reflectance of the Ba $(Zn_{1-x}Co_x)_2Si_2O_7$ (0 $\leq x \leq$ 0.50) samples were measured using a UV-Vis spectrometer (Shimadzu, UV-2550) with barium sulphate as a reference. The

Table 1 The compositions of the Ba($Zn_{1-x}Co_x$)₂Si₂O₇ (0 $\leq x \leq 0.50$) pigments

Stoichiometric composition	Analysed composition		
$BaZn_2Si_2O_7$	$Ba_{0.99}Zn_{1.99}Si_{2.02}O_{7.02}$		
$Ba(Zn_{0.95}Co_{0.05})_2Si_2O_7$	$Ba_{0.95}(Zn_{0.92}Co_{0.04})_2Si_{2.14}O_{7.15}$		
$Ba(Zn_{0.90}Co_{0.10})_2Si_2O_7$	$Ba_{1.04}(Zn_{0.87}Co_{0.11})_2Si_{2.00}O_{7.00}$		
$Ba(Zn_{0.85}Co_{0.15})_2Si_2O_7$	$Ba_{1.05}(Zn_{0.84}Co_{0.15})_2Si_{1.96}O_{6.96}$		
$Ba(Zn_{0.80}Co_{0.20})_2Si_2O_7$	$Ba_{0.94}(Zn_{0.81}Co_{0.22})_2Si_{2.00}O_{7.00}$		
$Ba(Zn_{0.75}Co_{0.25})_2Si_2O_7$	$Ba_{1.00}(Zn_{0.76}Co_{0.24})_2Si_{2.00}O_{7.00}$		
$Ba(Zn_{0.70}Co_{0.30})_2Si_2O_7$	$Ba_{1.05}(Zn_{0.71}Co_{0.29})_2Si_{2.14}O_{7.14}$		
$Ba(Zn_{0.65}Co_{0.35})_2Si_2O_7$	$Ba_{0.97}(Zn_{0.63}Co_{0.34})_2Si_{2.10}O_{7.10}$		
$Ba(Zn_{0.60}Co_{0.40})_2Si_2O_7$	$Ba_{0.95}(Zn_{0.58}Co_{0.37})_2Si_{2.15}O_{7.15}$		
$Ba(Zn_{0.55}Co_{0.45})_2Si_2O_7$	$Ba_{1.03}(Zn_{0.54}Co_{0.42})_2Si_{2.05}O_{7.05}$		
$Ba(Zn_{0.50}Co_{0.50})_2Si_2O_7$	$Ba_{1.00}(Zn_{0.51}Co_{0.47})_2Si_{2.05}O_{7.05}$		

colour properties of the samples were estimated in terms of the CIE $L^*a^*b^*Ch^\circ$ system using a calorimeter (Konica-Minolta, CR-300). This colour measurement was made for powder samples. In the case of the blue-violet pigment, positive a^* and negative b* values are desirable. Chroma parameter (C) represents the colour saturation of the pigments and is calculated according to the following formula: $C = [(a^*)^2 + (b^*)^2]^{1/2}$. The parameter h° ranges from 0 to 360° ($300 \le h^{\circ} \le 330$ means blue-violet), and is calculated with the formula, $h^{\circ} = \tan^{-1}(b^*/a^*)$.

Results and discussion

X-ray fluorescence analysis (XRF)

The XRF analysis data of the samples were listed in Table 1. All compositions were almost in good agreement with those of the nominal stoichiometric ones.

X-ray powder diffraction (XRD)

Fig. 1 shows the XRD patterns of the Ba $(Zn_{1-x}Co_x)_2Si_2O_7$ (0 $\leq x$ \leq 0.50) pigments. All samples were obtained in a single-phase form and the diffraction patterns were well indexed to that of the monoclinic BaZn₂Si₂O₇ structure whose space group was C2/c. ^{22,23,25} This structure is different from that of orthorhombic BaCu₂Si₂O₇ (ref. 26) having a similar composition. The diffraction peaks about 54° shifted to higher angles with increasing the Co^{2+} content. The lattice volumes of the $Ba(Zn_{1-r}Co_r)_2Si_2O_7$ $(0 \le x \le 0.50)$ samples calculated from the diffraction peaks are

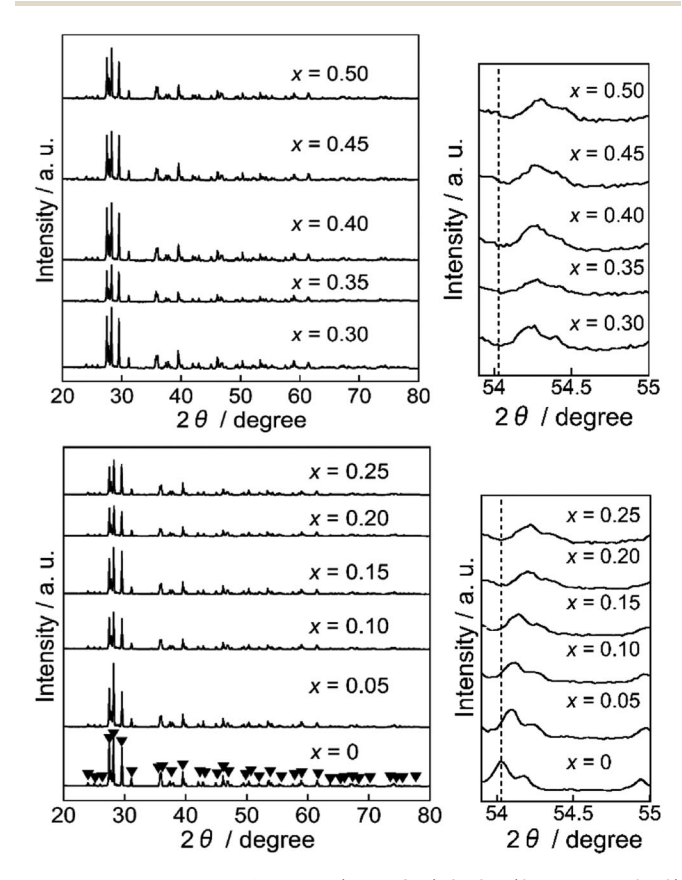


Fig. 1 XRD patterns of the $Ba(Zn_{1-x}Co_x)_2Si_2O_7$ (0 $\leq x \leq 0.50$) pigments.

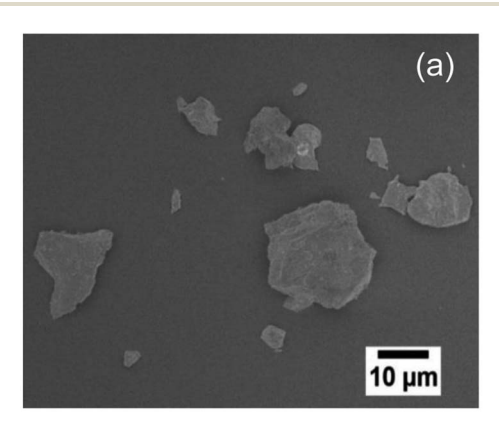
Table 2 Lattice volumes of the Ba($Zn_{1-x}Co_x$)₂Si₂O₇ (0 $\leq x \leq 0.50$) pigments

x	Lattice volume/ni		
	4.27600		
0	1.27603		
0.05	1.27570		
0.10	1.27559		
0.15	1.27555		
0.20	1.27497		
0.25	1.27463		
0.30	1.27449		
0.35	1.27383		
0.40	1.27370		
0.45	1.27356		
0.50	1.27330		

summarized in Table 2. The volume decreased with increasing the Co²⁺ concentration, indicating that the Zn²⁺ (ionic radius: 0.060 nm)²⁷ ions were partially substituted with the smaller Co²⁺ (ionic radius: 0.058 nm)27 ions and the solid solutions based on monoclinic BaZn₂Si₂O₇ were successfully synthesized in a single-phase form.

Scanning electron microscopic (SEM) image and energy dispersive X-ray (EDX) analysis

Fig. 2 depicts the SEM image and particle distribution of the Ba(Zn_{0.85}Co_{0.15})₂Si₂O₇ pigment. The average particle size calculated from 400 particles was about 13 µm. The EDX



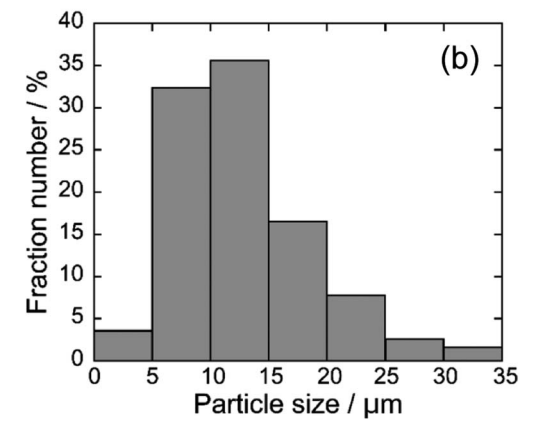


Fig. 2 SEM image (a) and particle distribution (b) of the $Ba(Zn_{0.85}$ -Co_{0.15})₂Si₂O₇ pigment.

analysis result for the Ba(Zn_{0.85}Co_{0.15})₂Si₂O₇ sample is shown in Fig. 3. It was confirmed that Ba, Zn, Si, Co and O were present and non-impurities were observed without Au (chargeup preventer). The X-ray dot mapping analysis results is depicted in Fig. 4, indicating that the component elements were uniformly distributed in the particle.

X-ray photoelectron spectrum (XPS)

The XPS of the $Ba(Zn_{0.85}Co_{0.15})_2Si_2O_7$ pigment is shown in Fig. 5. This spectrum was deconvoluted into three components, considering the spin-orbit doublets. The intense peaks at 795.3 eV and 780.2 eV were attributed to the Ba^{2+} $3d_{3/2}$ and $3d_{5/2}$ configurations, respectively.28,29 Although the small peaks observed at 793.7 eV and 778.6 eV were assigned to the Co³⁺ 2p_{3/2} and 2p_{1/2} lines, more intense peaks were also detected at 796.3 eV and 781.0 eV, corresponding to those of Co²⁺.29-31 These results indicate that the dominant oxidation state of cobalt ions was divalent on the surface of the Ba(Zn_{0.85}Co_{0.15})₂Si₂O₇ pigment. Furthermore, the d-d transition of the tetrahedral coordinated Co³⁺ ions was appeared around 9000 cm⁻¹ (1111 nm).³² Therefore, the Co3+ ions do not affect the colour of the present $Ba(Zn_{1-x}Co_x)_2Si_2O_7$ (0.05 $\leq x \leq$ 0.50) pigments.

Reflectance spectra

Fig. 6 depicts the UV-Vis diffuse reflectance spectra for the Ba(Zn_{1-r}Co_r)₂Si₂O₇ ($0 \le x \le 0.50$) pigments. High reflectance was observed in the visible light region for the Co²⁺-free $BaZn_2Si_2O_7$ (x=0) sample. On the other hand, strong absorption bands originated by the d-d transition of tetrahedral coordinated Co2+ (ref. 8, 33 and 34) were observed in the $Ba(Zn_{1-x}Co_x)_2Si_2O_7$ (0.05 $\leq x \leq$ 0.50) pigments from 550 to 650 nm corresponding to the green-orange lights. The Co²⁺ ion has the d⁷ electron configuration and the energy level structure of the Co²⁺ ion in a tetrahedral site is similar to that of d³ ion in an octahedral site.35 According to the Tanabe-Sugano diagram, the bands from 550 to 650 nm are assigned to the ${}^{4}A_{2}(F) \rightarrow$ ⁴T₁(P) transition of the tetrahedral coordinated Co²⁺. ³³⁻³⁶

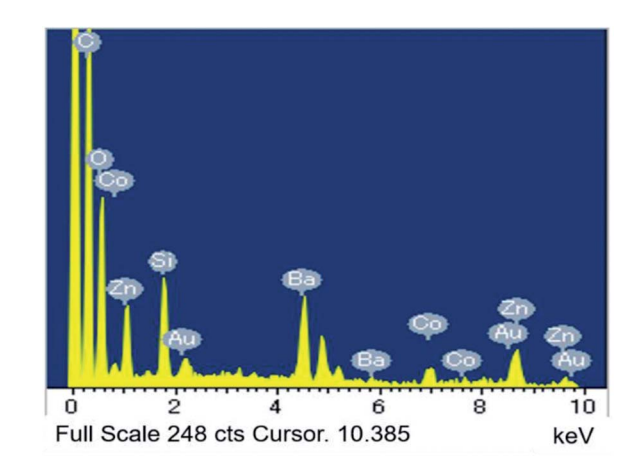


Fig. 3 The EDS analysis for Ba(Zn_{0.85}Co_{0.15})₂Si₂O₇.

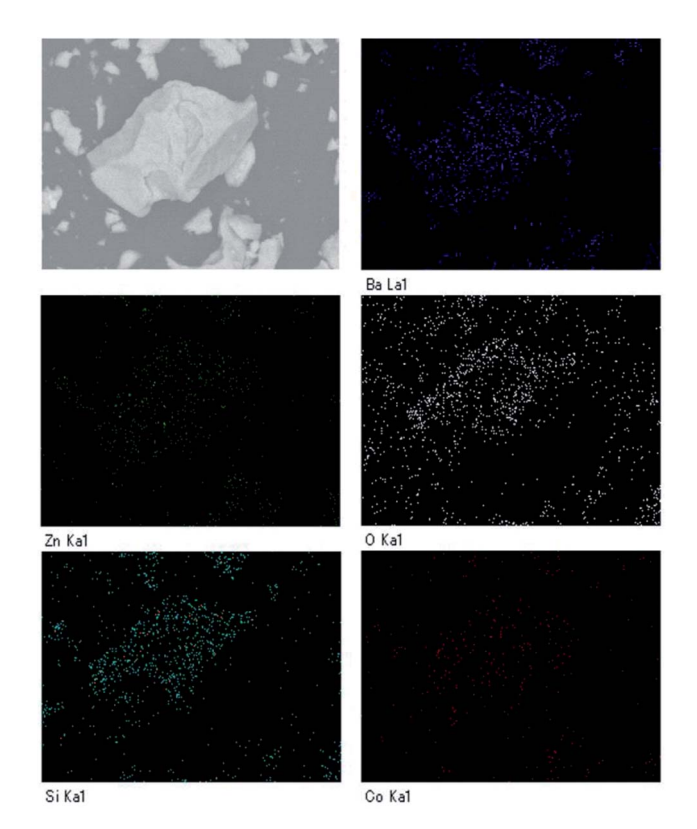


Fig. 4 The X-ray dot mapping analysis of the Ba(Zn_{0.85}Co_{0.15})₂Si₂O₇.

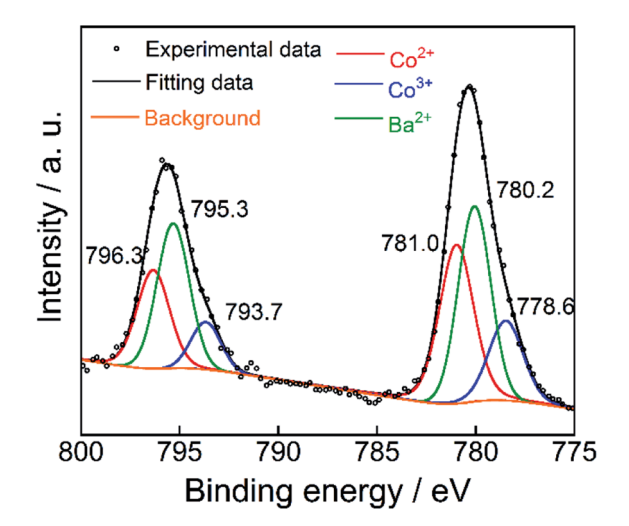


Fig. 5 XPS of Co 2p and Ba 3d on the surface of the Ba(Zn_{0.85}-Co_{0.15})₂Si₂O₇ pigment.

Chromatic properties

The $L^*a^*b^*Ch^\circ$ colour coordinate data for the Ba $(Zn_{1-x}Co_x)_2$ - Si_2O_7 ($0 \le x \le 0.50$) pigments are summarized in Table 3. They were compared using powder samples. It is obvious that the a^* and b^* values became significantly positive and negative, respectively, by the introduction of Co²⁺ in the host BaZn₂Si₂O₇ lattice. As mentioned in the previous section, the Ba(Zn_{1-x}-Co_x)₂Si₂O₇ pigments absorbed the green-orange lights but

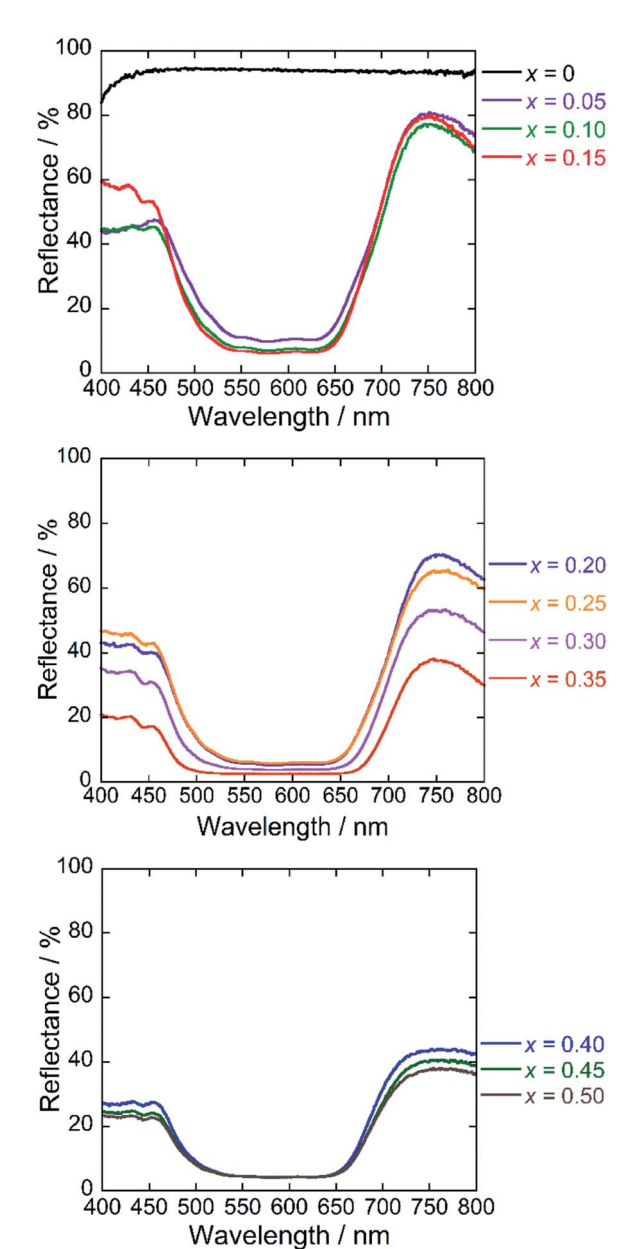


Fig. 6 UV-Vis reflectance spectra of the Ba($Zn_{1-x}Co_x$)₂Si₂O₇ ($0 \le x \le$ 0.50) pigments.

reflected the complementary blue and red lights. This is the reason for that positive a^* and negative b^* values were obtained in these pigments. The photographs of the Ba(Zn_{1-x}Co_x)₂Si₂O₇ $(0 \le x \le 0.50)$ samples are shown in Fig. 7. The colour of the $Ba(Zn_{1-x}Co_x)_2Si_2O_7$ (0 $\leq x \leq 0.50$) pigments gradually changed from white to dark blue-violet as the Co2+ concentration increased. Among the samples synthesized in this study, the largest absolute values in the colour coordinate data were obtained for Ba($Zn_{0.85}Co_{0.15}$)₂Si₂O₇ ($a^* = +52.2$ and $b^* = -65.5$).

They were compared with those of the commercially available Co₃(PO₄)₂ and NH₄MnP₂O₇ pigments in Table 4. It is notable that the absolute values of a^* and b^* for the Ba(Zn_{0.85}-Co_{0,15})₂Si₂O₇ were significantly larger than those for the commercial violet pigments.

Table 3 The $L^*a^*b^*Ch^\circ$ colour coordinates of the Ba($Zn_{1-x}Co_x$)₂Si₂O₇ (0 $\leq x \leq$ 0.50) pigments

x	L^*	a*	<i>b</i> *	C	h°
0	93.7	-0.01	+0.20	0.20	92.9
0.05	43.8	+27.9	-46.6	54.3	300.9
0.10	30.1	+39.8	-54.8	67.7	306.0
0.15	28.6	+52.2	-65.5	83.8	308.6
0.20	25.9	+44.9	-57.8	76.4	307.8
0.25	21.8	+49.9	-59.8	77.9	309.8
0.30	25.0	+33.3	-45.4	56.3	306.3
0.35	22.8	+27.4	-38.0	46.8	305.8
0.40	21.0	+35.9	-45.9	58.3	308.0
0.45	20.2	+33.4	-43.3	54.6	307.6
0.50	20.8	+30.4	-40.5	50.6	306.9

Chemical stability tests

The chemical stability of the Ba($\rm Zn_{0.85}Co_{0.15}$) $_2\rm Si_2O_7$ pigment was also evaluated using a powder sample. The pigment was soaked into 4% acetic acid and 4% ammonium bicarbonate. After leaving them at room temperature for 2 h, the pigments were washed with deionized water and ethanol, and then dried at room temperature. The colour of the pigment after the leaching test was evaluated using the calorimeter. As seen in Table 5, the colour of the present $\rm Ba(Zn_{0.85}Co_{0.15})_2Si_2O_7$ pigment was almost unchanged.

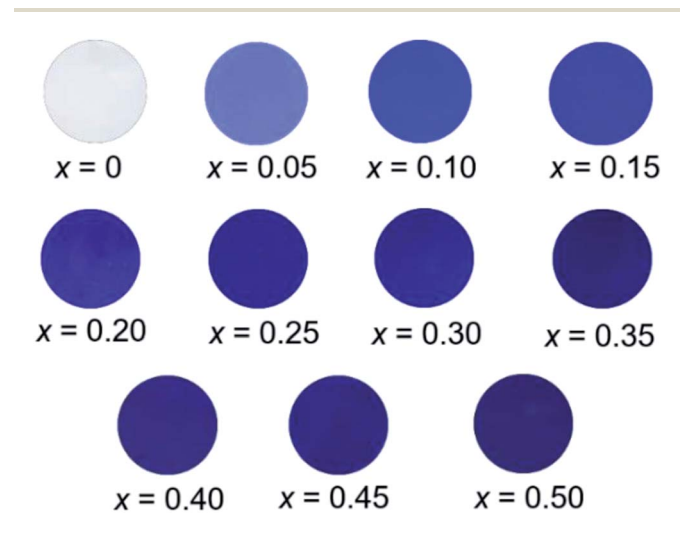


Fig. 7 Photographs of the $Ba(Zn_{1-x}Co_x)_2Si_2O_7$ (0 $\leq x \leq$ 0.50) pigments.

Table 4 The $L^*a^*b^*Ch^\circ$ colour coordinates of the Ba(Zn_{0.85}Co_{0.15})₂-Si₂O₇ pigment and commercial violet pigments

Samples	L^*	a*	<i>b</i> *	C	h°
Ba(Zn _{0.85} Co _{0.15}) ₂ Si ₂ O ₇	28.6	+52.2	-65.5	83.8	308.6
Co ₃ (PO ₄) ₂ ^a	46	+33	-32	44.3	315.9
NH ₄ MnP ₂ O ₇ ^a	31	+39	-21	46.0	331.7

^a Cited from ref. 20.

Table 5 The $L^*a^*b^*Ch^\circ$ colour coordinates of the Ba(Zn_{0.85}Co_{0.15})₂-Si₂O₇ pigment before and after the acid and base resistance tests

Pigment	L^*	a*	<i>b</i> *	C	h°
Non-treatment	28.6	+52.2	-65.5	83.8	308.6
4% CH ₃ COOH	28.0	+57.0	-69.4	89.8	309.4
4% NH ₄ HCO ₃	25.7	+56.2	-67.8	88.1	309.7

Conclusions

Ba $(Zn_{1-x}Co_x)_2Si_2O_7$ (0 $\leq x \leq 0.50$) solid solutions were successfully synthesized as novel blue-violet inorganic pigments. The samples strongly absorbed the visible light from 550 to 650 nm (green to orange), which was originated by the d-d transition of tetrahedrally coordinated Co^{2+} . Ba $(Zn_{0.85}Co_{0.15})_2Si_2O_7$ showed the most intense colour among the samples, and the $L^*a^*b^*Ch^\circ$ parameters were $L^*=28.6$, $a^*=+52.2$, $b^*=-65.5$, C=66.3, and $h^\circ=308.6$. The absolute values of a^* and b^* of Ba $(Zn_{0.85}Co_{0.15})_2Si_2O_7$ were significantly larger than those of the commercial $Co_3(PO_4)_2$ ($a^*=+33$ and $b^*=-32$) and $NH_4MnP_2O_7$ ($a^*=+39$ and $b^*=-21$) pigments. Furthermore, the Ba $(Zn_{0.85}Co_{0.15})_2Si_2O_7$ pigment has excellent chemical resistance and thermal stability. These results indicate that Ba $(Zn_{0.85}Co_{0.15})_2Si_2O_7$ could serve as an effective alternative to the conventional blue-violet inorganic pigments.

Conflicts of interest

There are no conflicts to declare.

Acknowledgements

This work was partially supported by JSPS KAKENHI Grant Number 15K05643. The authors thank Dr Hirokazu Izumi (Hyogo Prefectural Institute of Technology) for his assistance with the X-ray photoelectron spectroscopy measurement.

References

- 1 N. V. Russell, F. Wigley and J. Williamson, J. Mater. Sci., 2000, 35, 2131.
- 2 F. Miccichè, E. Oostveen, J. Van Haveren and R. Van Der Linde, *Prog. Org. Coat.*, 2005, 53, 99.
- 3 D. Uner, M. K. Demirkol and B. Dernaika, *Appl. Catal., B*, 2005, **61**, 334.
- 4 M. Frías and M. I. S. de Rojas, Cem. Concr. Res., 2002, 32, 435.
- 5 W. S. Cho and M. Kakihana, J. Alloys Compd., 1999, 287, 87.
- 6 K. Ullrich, O. Ott, K. Langer and K. D. Becker, *Phys. Chem. Miner.*, 2004, 31, 247.
- 7 L. C. K. De Souza, J. R. Zamian, R. G. N. da Filho,
 L. E. B. Soledade, I. M. G. Dos Santos, A. G. Souza,
 T. Scheller, R. S. Angélica and C. E. F. Da Costa, *Dyes Pigm.*, 2009, 81, 187.
- 8 J. Merikhi, H. O. Jungk and C. Feldmann, *J. Mater. Chem.*, 2000, **10**, 1311.

- 9 A. Shamirian, M. Edrisi and M. Naderi, *J. Mater. Eng. Perform.*, 2013, 22, 306.
- 10 S. Erič, L. Kostic-Gvozdenvić, M. Mirandinović and L. Pavlovič, *Ceram.-Silik.*, 1990, 34, 61.
- 11 M. Llusar, A. Forés, J. A. Badenes, J. Calbo, M. A. Tena and G. Monrós, *J. Eur. Ceram. Soc.*, 2001, **21**, 1121.
- 12 M. Llusar, A. Zielinska, M. A. Tena, J. A. Badenes and G. Monrós, J. Eur. Ceram. Soc., 2010, 30, 1887.
- 13 S. Meseguer, M. A. Tena, C. Gargor, J. A. Badenes, M. Llusar and G. Monrós, *Ceram. Interfaces*, 2007, 33, 843.
- 14 I. S. Ahmed, S. A. Shama, M. M. Moustafa, H. A. Dessouki and A. A. Ali, *Spectrochim. Acta, Part A*, 2009, 74, 665.
- 15 L. Robertson, M. Duttine, M. Gaudon and A. Demourgues, *Chem. Mater.*, 2011, 23, 2419.
- 16 N. Gorodylova, V. Kosinová, Ž. Dohnalová, P. Bělina and P. Šulcová, *Dyes Pigm.*, 2013, 98, 393.
- 17 D. Gryffroy, B. E. Vandenberghe and D. Poelman, *Solid State Commun.*, 1992, **82**, 497.
- 18 Y. Begum and A. J. Wright, J. Mater. Chem., 2010, 22, 21110.
- 19 A. E. Smith, H. Mizoguchi, K. Delaney, N. A. Spaldin, A. W. Sleight and M. A. Subramanian, J. Am. Ceram. Soc., 2009, 131, 17084.
- 20 S. W. Kim, Y. Saito, T. Hasegawa, K. Toda, K. Uematsu and M. Sato, *Dyes Pigm.*, 2017, **136**, 243.
- 21 Y. Chen, Y. Zhang and S. Feng, Dyes Pigm., 2014, 105, 167.
- 22 M. Kerstan, M. Müller and C. Rüssel, *J. Solid State Chem.*, 2012, **188**, 84.

- 23 J. H. Lin, G. X. Lu, J. Du, M. Z. Su, C. K. Loong and J. W. Richardson Jr, J. Phys. Chem. Solids, 1999, 60, 975.
- 24 C. Thieme and C. Rüssel, Dyes Pigm., 2014, 111, 75.
- 25 M. Krestan, C. Thieme, M. Grosch, M. Müller and C. Rüssel, I. Solid State Chem., 2013, 207, 55.
- 26 J. Janczak and R. Kubiak, Acta Crystallogr., Sect. C: Struct. Chem., 1990, 46, 1383.
- 27 R. D. Shannon, Acta Crystallogr., Sect. A: Cryst. Phys., Diffr., Theor. Gen. Crystallogr., 1976, 32, 751.
- 28 L. Wang, J. Zhang, Q. Zhang, N. Xu and J. Song, J. Magn. Magn. Mater., 2015, 377, 362.
- 29 B. Liu, Y. Zhang and L. Tang, Int. J. Hydrogen Energy, 2009, 34, 435.
- 30 J. Šponer, J. Čejka, J. Dědeček and B. Wichterlová, *Microporous Mesoporous Mater.*, 2000, 37, 117.
- 31 J. F. Marco, J. R. Gancedo, M. Gracia, J. L. Gautier, E. I. Ríos, H. M. Palmer, C. Greaves and F. J. Berry, *J. Mater. Chem.*, 2001, **11**, 3087.
- 32 D. L. Wood and J. P. Remeika, J. Chem. Phys., 1967, 46, 3595.
- 33 S. Meseguer, M. A. Tena, C. Gargori, R. Galindo, J. A. Badenes, M. Llusar and G. Monrós, *Ceram. Interfaces*, 2008, 34, 1431.
- 34 N. V. Kuleshov, V. P. Mikhailov, V. G. Scherbitsky, P. V. Prokoshin and K. V. Yumashev, *J. Lumin.*, 1993, **55**, 265.
- 35 A. K. Zvezdin and V. A. Kotov, *Modern Magnetooptics and Magnetooptical Materials*, CRC Press, 1993.
- 36 M. Dondi, C. Zanelli, M. Ardit and G. Cruciani, J. Am. Ceram. Soc., 2011, 94, 1025.